Journal of Building Engineering 91 (2024) 109645

Contents lists available at ScienceDirect

Journal of Building Engineering

journal homepage: www.elsevier.com/locate/jobe

Increasing the amorphous content in river sediments intended for supplementary cementitious materials using flame synthesis

Wolfgang Wisniewski [a,*], Jozef Kraxner [b], Lea Žibret [a], Dušan Galusek [b,c], Vilma Ducman [a]

[a] Slovenian National Building and Civil Engineering Institute (ZAG), Dimičeva 12, 1000 Ljubljana, Slovenia
[b] Centre for Functional and Surface Functionalized Glass, Alexander Dubcek University of Trenčín, 911 50 Trenčín, Slovakia
[c] Joint Glass Centre of the IIC SAS, TnUAD, and FChPT STU, 91150 Trenčín, Slovakia

ARTICLE INFO

Keywords:
Clay rich river sediments
Calcination
Flame synthesis
Reactivity
Supplementary cementitious materials (SCM)

ABSTRACT

Dredged river sediments are currently a waste material which is mainly landfilled or reintegrated into rivers. They can also be used as a renewable resource for the construction sector. Pre-treatments at high temperatures allow their use for more advanced applications such as supplementary cementitious materials (SCMs) or as a precursor for alkali activated materials (AAMs). The work presented here shows that flame synthesis can be used to almost completely vitrify such sediments and increase their leachability for Al and Si beyond the levels achieved by conventional calcination at 750–950 °C for 1h.

The reactivity of the prepared samples was analyzed via the Si and Al solubility in 10 M NaOH and was generally increased by the applied treatments but maximized by flame synthesis. Their microstructure was analyzed using scanning electron microscopy and their phase composition was monitored using X-ray diffraction. The results show an almost complete amorphization of the sediments by flame synthesis, however their reactivity does not increase at the same rate.

1. Introduction

Low carbon-footprint inorganic materials are constantly being sought after in the building sector, preferably if they can be produced using waste materials from local industries. Alkali activated materials (AAMs) [1–4] are discussed as one of the most promising material classes to meet this demand as 44–64 % reductions in greenhouse gas emission versus the reference material Ordinary Portland Cement (OPC) have been reported [5]. Other reports only conclude a 9 % emission reduction vs. OPC when a wide range of factors is taken into account [6], outlining why emissions must be minimized along the entire production chain. A more extensive comparison of CO_2 emissions for such materials in a recent review [4] shows a dramatic range of values: the stated values for OPC range from just above 100 to over 1200 kg CO_2/ton. The values for various AAMs are generally lower, but to very variable degrees, and in one case even surpass the OPC value. More importantly, it is emphasized that estimating the environmental performance should not be limited to CO_2 emissions but include a range of aspects [4]. The principal manufacture of AAMs is based on activating mainly amorphous aluminosilicates using alkaline activators such as NaOH or KOH, usually at temperatures below 100 °C [7].

The amorphous aluminosilicates used as precursors in AAMs are often also supplementary cementitious materials (SCMs) such as ground granulated blast furnace slag, fly ash, calcined clays, silica fume or natural pozzolans. However, the availability of SCMs is

* Corresponding author.
E-mail address: wolfgang.wisniewski@zag.si (W. Wisniewski).

https://doi.org/10.1016/j.jobe.2024.109645
Received 20 December 2023; Received in revised form 2 May 2024; Accepted 17 May 2024
Available online 17 May 2024

limited as they are frequently used to partially replace clinker or cement [8–10] for economic reasons so that a high proportion of suitable SCMs is already used in blended cements [10,11]. This limited supply and significant variations of the SCM properties in comparison to the property homogeneity of OPC [12] makes exploring alternative SCMs a constant focus of ongoing research [9].

While some raw materials can be directly used as SCMs, others require a pre-treatment such as calcination. Calcination has been reported to increase the amorphous content from less than 10 to more than 90 wt% [13–15], but of course this highly depends on the components of the raw material as some contain crystalline phases with high melting points such as quartz. Calcination, or heat treatments in general, should not be viewed as an automatic option for improvement as e.g. heating fly ash to 500 and 800 °C has been shown to decrease the amorphous content and the mechanical properties of AAMs based on it [16]. Calcined clays have already been used to produce AAMs [13,17–20]. Calcining clay causes three major phenomena in the usual temperature range from 100 to above 900 °C: dehydration, dehydroxylation, which is related to amorphization, and recrystallization [10,17]. Calcining clays for SCMs must be performed at an optimal temperature to maximize their reactivity because the latter is decreased by the recrystallization of thermodynamically stable phases at higher temperatures [10,14,17,20]. A review of clay materials used for AAMs up to 2019 was recently presented [10].

Given that a high amorphous content has been proven to play a vital role in alkali activation [21] and is considered to severely increase the reactivity of SCMs [10,14,20,22], a method known as "flame synthesis" could be relevant to the field of SCMs as it is used to produce completely amorphous microspheres from powders [23]. Flame synthesis is an innovative method developed for producing special glasses impossible to produce by classic procedures due to their high crystallization tendency [23–32]. During this process, e.g. illustrated by Dasan et al. [32], a precursor powder is shot into a gas flame where it melts to form droplets which are subsequently quenched with an extreme cooling rated due to their small size. The thus processed powder is highly amorphous but may contain some crystallized particles which either failed to fully melt in the flame or crystallized during cooling [27] as the flight path of the powder is impossible to control completely. The flame temperature and particle residence time in the flame are critical factors to the method because larger particles require a longer time to melt and assume the spherical shape. Amorphous microspheres of the åkermanite composition produced using flame synthesis have e.g. been used to stabilize bioactive scaffolds produced via additive manufacturing [33].

One group of raw materials suitable for flame synthesis are clay rich sediments from hydropower plant dams as they can show a favorable chemical composition and grain size distribution of below 200 μm in diameter [34]. As their sedimentation, excavation and deposition is a major problem worldwide, new solutions for using these sediments in different sectors from agriculture to the building industry are constantly sought. While such sediments have been successfully applied as raw materials in brick making [34] and show potential as soil stabilization materials [35], their performance in AAMs for building components has been insufficient so far unless reactive additives such as slag or fly ash are added [35]. One approach to turn these sediments into SCMs is to increase the solubility of Si^{4+} because it enters into the pozzolanic reaction with the portlandite ($Ca(OH)_2$) from cements to produce a $CaO–SiO_2–H_2O$ (C–S–H) gel which, however, differs significantly from the C–S–H gel formed in OPC [36]. Increasing their amorphous content could increase this solubility and hence upgrade the sediments to SCMs suitable for the alkali activation process, opening new possibilities for application in higher added value products.

The aim of the work presented here is to use calcination and flame synthesis to maximize the amorphous content of the previously analyzed sediments and to assess the reactivity of the thus obtained powders for further potential use in SCM production. In contrast to calcination, the high temperatures achieved by flame synthesis can melt thermodynamically stable phases such as cristoballite or mullite, and lead to a full amorphization of possibly suitable sediments.

2. Materials & methods

A fresh and an aged sediment from the Drava river (Slovenia) [35] were used as raw materials. Their loss on ignition (LOI) was determined by respectively heating ca. 3–4 g of each sediment to 950 °C where they were held for 2 h after drying them to a constant mass in an IR moisture analyser (Mettler Toledo, HE73) at 105 °C. The resulting materials were mixed with Fluxana (Li-tetraborate and Li-metaborat mixed in a mass ratio of 1:1) at a ratio of 1:10 and melted into discs. $LiBr_{(l)}$ (50 mL H_2O and 7.5 g of $LiBr_{(s)}$ from Sigma Aldrich) was added to the mixture to prevent the melt from sticking to the Pt crucible. The chemical compositions were then determined using an ARL PERFORM'X sequential X-ray fluorescence (XRF) spectrometer (Thermo Fisher Scientific Inc., Ecublens, Switzerland) using the UniQuant 5 software (Thermo Fisher Scientific Inc., Walthem, MA, USA).

The fresh and aged sediments were dried in a Kambic SP-440 laboratory oven at 60 °C before batches of approximately 20 g were calcined in alumina crucibles in a Nabertherm N 11/HR furnace by heating them to 750, 850 or 950 °C with a heating rate of 5 K/min where they dwelled for 1 h before they were removed from the furnace and cooled in air.

The raw materials for flame synthesis were crushed in an agate mortar and sieved into batches with particle sizes of either <63 μm or <100 μm. The sieved powders were flame synthesized using a laboratory device based at the FunGlass Centre in Trencin, Slovakia approved as a utility model [31]. Here a vacuum powder feeder provides the powders to a flame of ~2100 °C running with a CH_4/O_2 gas mixture at a rate of 3.0 g min^{-1}. The powders pass through the flame along its long axis, melt, and form droplets immediately quenched in a spray of deionized water. The obtained microspheres were collected in a water-filled tank and extracted by filtration using a ceramic microfilter with a porosity of less than 0.3 μm. The collected batches were heated to 650 °C for 4 h to remove any organic residue or carbon (soot) which can result from slight imperfections in the burner gas mixture.

The phase composition of the prepared powders was analyzed using X-ray diffraction (XRD) in the Bragg-Brentano configuration using PANalytical Empyrean X-ray powder diffractometers operating with Cu anodes (Cu $K_{\alpha1,}$ (8047.8162(4) eV) and Cu $K_{\alpha2}$ (8027.9435(2) eV) and an accelerating voltage of 45 kV. Spectra were acquired from $10° < 2\Theta < 60°$ at a step size of 0.026°.

Table 1
Chemical composition of fresh and aged sediments measured using XRF. Note that the LOI content is considered to be additional as it was measured before the XRF analyses were performed.

content [wt.%]	fresh sediment	aged sediment
SiO_2	55.6	54.8
Al_2O_3	17.9	18.4
Fe_2O_3	6.3	6.7
CaO	7.8	7.5
MgO	5.9	6.0
Na_2O	1.6	1.5
K_2O	2.6	2.8
other	2.3	2.3
LOI (950 °C)	14.3	14.5

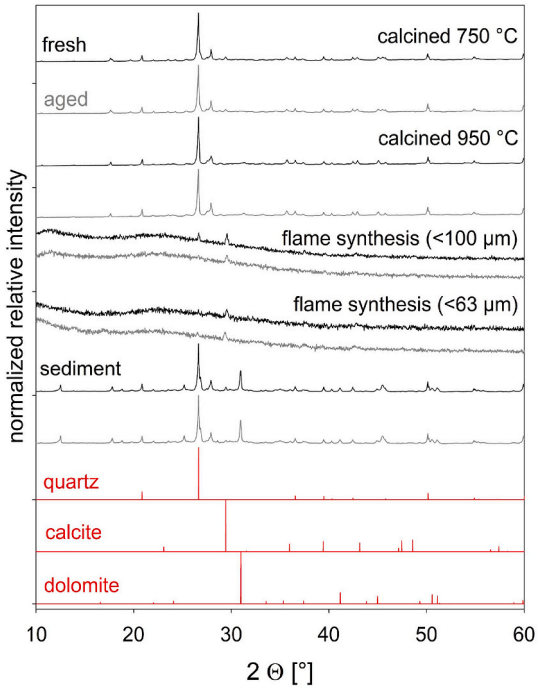

Fig. 1. XRD patterns acquired from fresh and aged sediments as well as before and after flame synthesis and calcination at the respectively stated temperatures for 1h. The theoretical patterns of quartz (ICSD 27831), calcite (ICSD 18166) and dolomite (ICSD 66333) are presented for comparison.

Scanning electron microscopy (SEM) was performed using a JSM-IT500 (Jeol, Tokyo, Japan) in low vacuum mode. Energy dispersive X-ray spectroscopy (EDXS) was performed using an Ultim Max 65 detector (Oxford Instruments, Abingdon, UK) and the software Aztec 5.0 (Oxford Instruments, Abingdon, UK). SEM figures and EDXS maps were acquired using an acceleration voltage of 20 kV. Optical micrographs were acquired using an optical microscope Nikon Eclipse ME 600 (Nikon, Tokyo, Japan).

The specific surface area of samples sieved to a grain size below 63 µm and dried in a laboratory oven at 105 °C for 20 h was measured using nitrogen adsorption. 1.5 g of each sample were analyzed via the Brunauer–Emmet–Teller (BET) method in an ASAP-2020 (Micromeritics, Norcross, GA, USA).

The dissolution of Si and Al from selected powders was determined using a Varian 715-ES ICP Optical Emission Spectrometer (Agilent HP). The samples were sieved to a grain size below 63 µm and 1.0 (±0.0001) g were mixed with 40 mL of 10 M NaOH for 24 h under continuous stirring [37]. The pH values of the solutions were reduced to values below 2.0 by adding concentrated (65 wt%) HNO_3.

The strength activity index (SAI) was determined using two experiments including CEM I cement. The calcined sediments and a fresh FS-treated sediment were tested after 28 and 90 days according to SIST EN 450-1 [38]. The sample/cement ratio was 25 : 75 wt%. The mortar was prepared following SIST EN 196-1 (Methods of testing cement) using 225 g of sediment, 125 g of water and 675 g of sand. The remaining SAI tests of FS-treated sediments and a silica reference were performed according to EN 13263-1 [39] where the sample/cement ratio was 10 : 90 wt%.

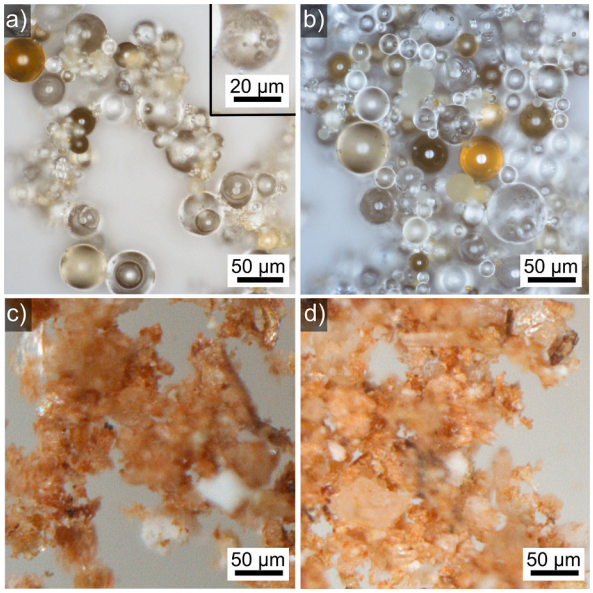

Fig. 2. Optical micrographs of the a) aged or b) fresh sediments after flame synthesis as well as c) aged or d) fresh sediments after calcination at 950 °C for 1h and sieved to grain sizes below 125 µm.

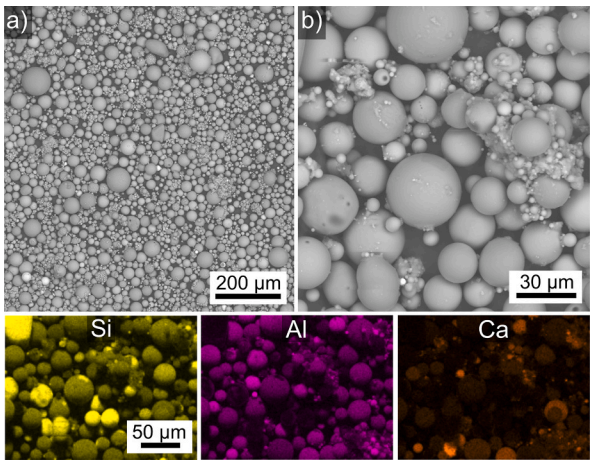

Fig. 3. SEM micrographs featuring a) an overview of the aged sediment after flame synthesis and b) the same batch in greater detail. Selected EDXS element maps are presented below.

3. Results

The sediments were analyzed using XRF and their chemical compositions are summarized in Table 1 along with the measured LOI. The values of the fresh and aged sediments are in acceptable agreement with previous measurements [35].

These sediments were statically calcined for 1 h as well as processed by flame synthesis. Fig. 1 presents XRD-patterns acquired from the fresh and aged sediments after calcination at the respectively stated temperatures or after flame synthesizing the respectively stated grain size fractions. XRD-patterns of the fresh and aged sediments are presented below for comparison. The untreated sediments were previously shown to mainly contain the minerals quartz (~25 wt%), illite (~15 wt%, a group of interlayer-deficient micas with non-expandable layers [17]), feldspar (~12 wt%) and dolomite (~14 wt%) [35]. After calcination, the peaks at e.g. $2\Theta \approx 32°$ are no longer observed, indicating the decomposition of dolomite. The peak at $2\Theta \approx 26°$ discernible after flame synthesizing the <100 µm grain size of the fresh sediment corresponds to the 100%-peak of the theoretical quartz pattern presented below. The peak at $2\Theta \approx 29°$ discernible in all presented patterns acquired after FS matches the 100 % peak of calcite which is barely discernible in the untreated river sediments and not discernible in the calcined river sediments. As calcite ($CaCO_3$, melting point 1339 °C) is unlikely to remain crystalline during a process where significant amounts of quartz (SiO_2, melting point above 1600 °C) are melted, any calcite detected after flame synthesis should result from a reaction after passing through the flame. CaO can result from the sediment decomposition and react with water to form $Ca(OH)_2$, which in turn can react with CO_2 from the air, burned gas or dissolved in water to yield $CaCO_3$.

Table 2
Dissolution of Al and Si and the specific surface measured using the BET method for the respective raw materials.

10 mol NaOH	dissolution [mg/L]			BET
24h at RT	grain size	Al	Si	m^2/g
* = fresh sediment	**<63 μm**	46	115	5.6
# = aged sediment	**<63 μm**	54	134	6.1
* calcined 750 °C	**<63 μm**	157	572	4.5
# calcined 750 °C	**<63 μm**	169	581	4.9
* calcined 850 °C	**<63 μm**	155	546	3.4
# calcined 850 °C	**<63 μm**	159	568	3.4
* calcined 950 °C	**<63 μm**	121	441	2.2
# calcined 950 °C	**<63 μm**	121	438	2.0
* flame synthesized	**<63 μm**	283	707	2.9
# flame synthesized	**<63 μm**	337	897	8.5
* flame synthesized	**as produced**	282	670	3.1
# flame synthesized	**as produced**	356	907	9.2

Another weak peak at $2\Theta \approx 28^{\circ}$ probably attributable to feldspar is still observed after calcination but not after flame synthesis. Hence the sediments were almost completely vitrified to an XRD amorphous level by flame synthesis, i.e. the crystalline content should be below 1 vol%.

The color and transparency of the FS treated river sediments is visualized in Fig. 2. The flame synthesized powders are composed of transparent spheres ranging from a few μm to almost 50 μm in diameter and colors from yellow/brown to colorless as shown in Fig. 2. The inset in Fig. 2 a) highlights a sphere containing what appear to be numerous bubbles which could result from gasses released during melting but then trapped in the rapidly cooled melt. The smaller spheres form agglomerates. Micrographs of the sediments after calcination at 950 °C and sieved to grain sized below 125 μm are presented below for comparison. They also form agglomerates and seem to contain a comparably large fraction of very small particles whereas particles appearing to be larger than 20 μm in diameter seem to be rather rare.

The overview of particle shapes in Fig. 3 a) shows that some spheres reach sizes beyond 50 μm in diameter. The more detailed micrograph in Fig. 3 b) shows that there are also many small particles less than 5 μm in diameter. The EDXS element maps of Si, Al and Ca acquired from this area show that some spheres show heterogeneous chemical compositions, e.g. local enrichments of Si. At this point it should be noted that neither EDXS measurements nor SEM micrographs are suited to actually prove crystallinity as implied in Ref. [21], meaning such analyses heavily depend on the defined segmentation criteria. While this can be correct to with some probability, proving crystallinity using electron microscopy depends on diffraction based methods such as EBSD [27]. As minerals such as illite and feldspar can show a wide range of chemical compositions, attributing the flame synthesized spheres to previous minerals is impossible. However, the chemical heterogeneities within the measured spheres indicated that melt droplets formed from different minerals combined to form larger droplets during flame synthesis to minimize their surface.

Previous analyses of the SCM reactivity based on the dissolution of Si and Al in NaOH or KOH showed that the maximum dissolution was generally achieved using the most alkaline concentration of NaOH (10 mol) for the maximum time of 24 h [37]. Applying this procedure to the untreated, calcined or flame synthesized raw materials led to the results presented in Table 2. They show that calcination significantly enhances the dissolution of both elements reaching a maximum when calcined at 850 °C which is in agreement with the literature [17]. Applying FS and testing the dissolution of a comparable grain size fraction more or less doubled the dissolution of Al in both aged and fresh sediments and significantly enhanced the dissolution of Si, especially when applied to the aged sediment which shows a higher relative content of SiO_2 in the form of quartz [34]. The dissolution of unsieved FS-treated sediments (as produced) led to very similar results, confirming these results but also indicating that the larger particles removed by sieving do not have a large effect on the leachability of Al and Si. The specific surface of the respective powders decreased with increasing calcination temperatures. The value for fresh FS sediment, sieved or not, is close to that after calcination at 850 °C while that for the aged FS sediment is significantly larger. Additionally, the as produced flame synthesized sediments show slightly larger specific surface values then when this material is crushed and sieved.

The most important result here is that the fresh FS-treated sediment crushed and sieved to grain sizes below 63 μm shows a much higher dissolution of Al and Si than the sample calcined at 850 °C despite having a smaller specific surface. This is in agreement with the concept that a higher amorphous content increases the leachability of these elements. The much higher specific surface of the aged sediments after FS also sufficiently explains the elevated leaching results measured for these samples in comparison to the fresh sediment.

However the BET results of the FS treated sediments show two counterintuitive aspects: i) the crushed and smaller particles should have a higher specific surface than compact spheres resulting from the FS process and ii) the more than doubled specific surface of the aged sediment after FS cannot easily be explained by the elevated quartz content in the aged sediment [34]. While some of the spheres resulting from FS clearly contain bubbles, see inset in Fig. 2 a), such a large increase would rather match the presence of a foaming agent in the aged sediment. Crushing such bubbles could lead to a larger amount of very fine powder which could agglomerate, affectively decreasing the specific surface of the material. Both of these observations likely require a more detailed understanding of the aging process for sediments than is currently available.

The pozzolanic properties of three calcined sediments and one batch of fresh FS treated sediment were respectively analyzed by

Table 3
SAI results of obtained from river sediments after the respectively stated treatment as well as values from a silica reference measured for comparison. # according to SIST EN 450-1 or * according to EN 13263-1.

treatement	SAI (28 days)	SAI (90 days)
calcined at 700 °C for 1h #	72.1 %	77.3 %
calcined at 850 °C for 1h #	72.7 %	64.8 %
calcined at 900 °C for 1h #	65.4 %	66.7 %
FS fresh sediment (as produced)#	63.3 %	57.8 %
FS fresh sediment (as produced)*	76.0 %	not required
FS aged sediment (as produced)*	79.0 %	not required
silica reference*	134 %	not required

determining their strength activity index (SAI) according to SIST EN 450-1 [38,40]: it must reach at least 75 % after 28 days and at least 85 % after 90 days for a material to be classified as a pozzolanic additive. The remaining SAI measurements for FS treated sediments and a silica reference were performed according to EN 13263-1 [39] because it requires a smaller amount of raw materials. Here the SAI must reach at least 100 % after 28 days. The results stated in Table 3 show that both the performed calcination procedure and flame synthesis failed to sufficiently enhance the sediments for this application: the value of commercial silica fume, classified as a pozzolanic additive, is presented as a reference. Hence both treatments also fail to upgrade these sediments as SCMs where a minimum of 100 % is required [39]. The BET values in Table 3 show that both treatments also fail to achieve the required values of 15–35 m^2/g for an SCM [39] whereas a commercial silica reference measured for comparison reached 23.8 g/m^2.

In summary, the FS treatment successfully maximized the amorphous content of the sediments. Although this treatment pushed the leachability of Al and Si from the analyzed river sediments beyond the values achieved by calcination, it failed to reach the levels required to upgrade these raw materials to SCMs.

While using flame synthesis based on CH_4/O_2 at a scale suitable to process thousands of tons per year would probably negate any environmental benefits provided by upgrading comparable raw materials to suitable SCMs at this time, using an environmentally friendly source of fuel such as "green" H_2 can make this process and a viable CO_2 free alternative in the future. Hence suitable sediments extracted at e.g. hydropower plants should be deposited and cataloged as future raw materials. Furthermore, sediment aging actually appears to improve the results of the presented process. Hence an more detailed understanding of the aging process can become relevant if this observation turns out to be systematic.

4. Conclusions

Clay rich sediments were calcined and treated by flame synthesis to increase their amorphous content. While calcination only increased the amorphous content slightly, flame synthesis allowed an almost complete vitrification. The most comparable FS-treated sample showed a higher leachability than its calcined counterpart despite having a smaller specific surface, supporting the significance of the amorphous content to the leachability. Aging a sediment is indicated to benefit the presented process.

Flame synthesis is a suitable method to maximize the amorphous content in raw materials possibly suited as precursors in SCMs or AAMs. However, it also changes the particle morphology to spheres, so its utility should be tested case by case. Preparing small amounts of material using FS enables to quickly test the maximum solubility in ~100 % amorphous materials.

Funding

This research was funded by the Slovenian Research Agency (ARRS) via project L7-2629: "Evaluation and remediation of sediments for further use in building sector (READY4USE)".

CRediT authorship contribution statement

Wolfgang Wisniewski: Writing – review & editing, Writing – original draft, Conceptualization. **Jozef Kraxner:** Methodology, Formal analysis. **Lea Žibret:** Methodology, Formal analysis. **Dušan Galusek:** Writing – review & editing, Supervision, Conceptualization. **Vilma Ducman:** Writing – review & editing, Supervision, Funding acquisition, Conceptualization.

Declaration of competing interest

The authors declare that they have no known competing financial interests or personal relationships that could have appeared to influence the work reported in this paper.

Data availability

Data will be made available on request.

Acknowledgments

We thank our colleagues at the ZAG Laboratory for Cements, Mortars and Ceramics for their technical support.

References

[1] D. Khale, R. Chaudhary, Mechanism of geopolymerization and factors influencing its development: a review, J. Mater. Sci. 42 (2007) 729–746, https://doi.org/10.1007/s10853-006-0401-4.

[2] J.L. Provis, A. Palomo, C. Shi, Advances in understanding alkali-activated materials, Cem. Concr. Res. 78 (2015) 110–125, https://doi.org/10.1016/j.cemconres.2015.04.013.

[3] J.L. Provis, Alkali-activated materials, Cem. Concr. Res. 114 (2018) 40–48, https://doi.org/10.1016/j.cemconres.2017.02.009.

[4] A. Dacic, K. Kopecskó, O. Fenyvesi, I. Merta, The obstacles to a broader application of alkali-activated binders as a sustainable alternative—a review, Materials 16 (2023) 3121, https://doi.org/10.3390/ma16083121.

[5] B.C. McLellan, R.P. Williams, J. Lay, A. van Riessen, G.D. Corder, Costs and carbon emissions for geopolymer pastes in comparison to ordinary portland cement, J. Clean. Prod. 19 (2011) 1080–1090, https://doi.org/10.1016/j.jclepro.2011.02.010.

[6] L.K. Turner, F.G. Collins, Carbon dioxide equivalent (CO2-e) emissions: a comparison between geopolymer and OPC cement concrete, Constr. Build. Mater. 43 (2013) 125–130, https://doi.org/10.1016/j.conbuildmat.2013.01.023.

[7] J. Davidovits, Geopolymers: ceramic-like inorganic polymers, J. Ceram. Sci. Technol. 8 (2017) 335–350, https://doi.org/10.4416/JCST2017-00038.

[8] M.C.G. Juenger, R. Snellings, S.A. Bernal, Supplementary cementitious materials: new sources, characterization, and performance insights, Cem. Concr. Res. 122 (2019) 257–273, https://doi.org/10.1016/j.cemconres.2019.05.008.

[9] M.C.G. Juenger, R. Siddique, Recent advances in understanding the role of supplementary cementitious materials in concrete, Cem. Concr. Res. 78 (2015) 71–80, https://doi.org/10.1016/j.cemconres.2015.03.018.

[10] A.Z. Khalifa, Ö. Cizer, Y. Pontikes, A. Heath, P. Patureau, S.A. Bernal, A.T.M. Marsh, Advances in alkali-activation of clay minerals, Cem. Concr. Res. 132 (2020) 106050, https://doi.org/10.1016/j.cemconres.2020.106050.

[11] F. Avet, R. Snellings, A.A. Diaz, M.B. Haha, K. Scrivener, Development of a new rapid, relevant and reliable (R3) test method to evaluate pozzolanic reactivity of calcined kaolinitic clays, Cem. Concr. Res. 85 (2016) 1–11, https://doi.org/10.1016/j.cemconres.2016.02.015.

[12] R. Snellings, K.L. Scrivener, Rapid screening tests for supplementry cementitious materials: past and future, Mater. Struct. 49 (2016) 3265–3279, https://doi.org/10.1617/s11527-015-0718-z.

[13] K. Traven, B. Horvat, M. Češnovar, M. Božič, B. Gregorc, V. Ducman, Reactivity of calcined river sediments. V: Sediment challenges and opportunities due to climate change and sustainable development : 12th International SedNet Conference : *online : 28 June - 2 July 2021*. Utrecht: SedNet. 2021, str. 1, ilustr. https://sednet.org/wp-content/uploads/2021/07/Abstr-CE-2.17.-POSTER-K.-Traven.pdf, https://cdn-assets.inwink.com/a369b015-a901-4e02-b66b-a43abe171f0f/ff39ba59-2821-4628-be73-2bdc6dd1a05a.

[14] S.C. Taylor-Lange, E.L. Lamon, K.A. Riding, M.C.G. Juenger, Calcined kaolinite–bentonite clay blends as supplementary cementitious materials, Appl. Clay Sci. 108 (2015) 84–93, https://doi.org/10.1016/j.clay.2015.01.025.

[15] A. Nikolov, H. Nugteren, I. Rostovsky, Optimization of geopolymers based on natural zeolite clinoptilolite by calcination and use of aluminate activators, Constr. Build. Mater. 243 (2020) 118257, https://doi.org/10.1016/j.conbuildmat.2020.118257.

[16] J. Temuujin, A. van Riessen, Effect of fly ash preliminary calcination on the properties of geopolymer, J. Hazard Mater. 164 (2009) 634–639, https://doi.org/10.1016/j.jhazmat.2008.08.065.

[17] T. Hanein, K.-C. Thienel, F. Zunino, A.T.M. Marsh, M. Maier, B. Wang, M. Canut, M.C.G. Juenger, M.B. Haha, F. Avet, A. Parashar, L.A. Al-Jaberi, R.S. Aares-Reyes, A. Alujas-Diaz, K.L. Scrivener, S.A. Bernal, J.L. Provis, T. Sui, S. Bishnoi, F. Martirena-Hernández, Clay calcination technology: state-of-the-art review by the RILEM TC 282-CCL, Mater. Struct. 55 (2022) 3, https://doi.org/10.1617/s11527-021-01807-6.

[18] N. Essaidi, B. Samet, S. Baklouti, S. Rossignol, Feasibility of producing geopolymers from two different Tunisian clays before and after calcination at various temperatures, Appl. Clay Sci. 88–89 (2014) 221–227, https://doi.org/10.1016/j.clay.2013.12.006.

[19] C. Ferone, B. Liguori, I. Capasso, F. Colangelo, R. Cioffi, E. Cappelletto, R. DiMaggio, Thermally treated clay sediments as geopolymer source material, Appl. Clay Sci. 107 (2015) 195–204, https://doi.org/10.1016/j.clay.2015.01.027.

[20] A. D'Elia, D. Pinto, G. Eramo, L.C. Giannossa, G. Ventruti, R. Laviano, Effects of processing on the mineralogy and solubility of carbonate-rich clays for alkaline activation purpose: mechanical, thermal activation in red/ox atmosphere and their combination, Appl. Clay Sci. 152 (2018) 9–21, https://doi.org/10.1016/j.clay.2017.11.036.

[21] Liu, J.-H. Doh, D.E.L. Ong, Z. Liu, M.N.S. Hadi, Methods to evaluate and quantify the geopolymerization reactivity of waste-derived aluminosilicate precursor in alkali-activated material: a state-of-the-art review, Constr. Build. Mater. 362 (2023) 129784, https://doi.org/10.1016/j.conbuildmat.2022.129784.

[22] A. Shvarzman, K. Kovler, G.S. Grader, G.E. Shter, The effect of dehydroxylation/amorphization degree on pozzolanic activity of kaolinite, Cem. Concr. Res. 33 (2003) 405–416, https://doi.org/10.1016/s0008-8846(02)00975-4.

[23] M. Mahmoud, J. Kraxner, H. Elsayed, E. Bernardo, D. Galusek, Fabrication and environmental applications of glass microspheres: a review, Ceram. Int. 49 (2023) 39745–39759, https://doi.org/10.1016/j.ceramint.2023.10.040.

[24] A. Prnová, R. Karell, D. Galusek, Al2O3–Y2O3 binary glass microspheres: synthesis and characterisation, Adv. Mater. Res. 39–40 (2008) 189–192, https://doi.org/10.4028/www.scientific.net/AMR.39-40.189.

[25] G. He, G. Liu, S. Guo, Z. Yang, J. Li, Crystallization of $Y_3Al_5O_{12}$:Ce^{3+} glass microspheres prepared by flame-spraying synthesis, J. Mater. Sci. Mater. Electron. 26 (2015) 72–77, https://doi.org/10.1007/s10854-014-2365-5.

[26] A. Prnová, A. Plško, J. Valúchová, P. Švančárek, R. Klement, M. Michálková D. Galusek, Crystallization kinetics of yttrium aluminate glasses, J. Therm. Anal. Calorim. 133 (2018) 227–236, https://doi.org/10.1007/s10973-017-6948-2.

[27] W. Wisniewski, P. Švančárek, A. Prnová, M. Parchovianský, D. Galusek, Y_2O_3–Al_2O_3 microsphere crystallization analyzed by electron backscatter diffraction (EBSD), Sci. Rep. 10 (2020) 11122, https://doi.org/10.1038/s41598-020-67816-7.

[28] M. Majerová, A. Dvurečenskij, A. Cigáň, M. Škrátek, A. Prnová, J. Kraxner, D. Galusek, J. Maňka, Magnetic properties of synthetic gehlenite glass microspheres, Acta Phys. Pol., A 131 (2017) 699–701.

[29] E. Bernardo, L. Fiocco, A. Prnová, R. Klement, D. Galusek, Gehlenite:Eu^{3+} phosphors from a silicone resin and nano-sized fillers, Opt. Mater. 36 (2014) 1243–1249.

[30] S.-J. Shih, Y.-C. Lin, S.-H. Lin, P. Veteška, D. Galusek, W.-H. Tuan, Preparation and characterization of Eu-doped gehlenite glassy particles using spray pyrolysis, Ceram. Int. 42 (2016) 11324–11329.

[31] J. Kraxner, V. Masár, S. Timár, J. Chovanec, Utility Model No. 8673, Zariadenie Na Výrobu Plných, Dutých Alebo Pórovitých Sklených Alebo Sklo-Keramických Mikroguľôčok Pomocou Plameňovej Syntézy, Slovakia, 2020.

[32] A. Dasan, A. Talimian, J. Kraxner, Dušan Galusek, H. Elsayed, E. Bernardo, Åkermanite glass microspheres: preparation and perspectives of sinter-crystallization, Int. J. Appl. Glass Sci. 12 (2021) 551–561, https://doi.org/10.1111/ijag.16115.

[33] J. Kraxner, H. Elsayed, A. Dasan, M. Hujová, M. Michálková, M. Michálek, E. Bernardo, D. Galusek, Additive manufacturing of Ca–Mg silicate scaffolds supported by flame-synthesized glass microspheres, Ceram. Int. 48 (2022) 9107–9113, https://doi.org/10.1016/j.ceramint.2021.12.095.

[34] K.F. Bizjak, B. Likar, M. Kolar, A. Robba, J. Imperl, M. Božič, B. Gregorc, V. Ducman, Evaluation of sediments from the river Drava and their potential for further use in the building sector, Materials 15 (2022) 4303, https://doi.org/10.3390/ma15124303.

[35] L. Žibret, W. Wisniewski, B. Horvat, M. Božič, B. Gregorc, V. Ducman, Clay rich river sediments calcined into precursors for alkali activated materials, Appl. Clay Sci. 234 (2023) 106848, https://doi.org/10.1016/j.clay.2023.106848.

[36] B. Lothenbach, K. Scrivener, R.D. Hooton, Supplementary cementitious materials, Cem. Concr. Res. 41 (2011) 1244–1256, https://doi.org/10.1016/j.cemconres.2010.12.001.

[37] C. Panagiotopoulou, E. Kontori, T. Perraki, G. Kakali, Dissolution of aluminosilicate minerals and by-products in alkaline media, J. Mater. Sci. 42 (2007) 2967–2973, https://doi.org/10.1007/s10853-006-0531-8.

[38] EN 450-1, Fly Ash for Concrete – Part 1: Definition, Specifications and Conformity Criteria, 2012.
[39] EN 13263-1:2005+A1:2009: Silica Fume for Concrete - Part 1: Definitions, Requirements and Conformity Criteria.
[40] S. Kramar, V. Ducman, Evaluation of ash pozzolanic activity by means of the strength activity index test, frattini test and DTA/TG analysis, Teh. Vjesn. 25 (2018) 1746–1752, https://doi.org/10.17559/TV-20171203193229.